

# GRAPHICAL THERMAL MODEL OF PROTON EXCHANGE MEMBRANE FUEL CELL SYSTEM BASED ON ENERGETIC MACROSCOPIC REPRESENTATION

Rui Pan, Duo Yang, Yujie Wang, Zonghai Chen\*

Department of Automation, University of Science and Technology of China, Hefei, China

## ABSTRACT

The fuel cell is actually an energy conversion device which converts Gibbs free energy of reactants into electrical energy. And the remaining enthalpy changes and chemical overpotential loss will generate a lot of heat. However, the performance of fuel cell is strongly dependent on the operation temperature, therefore it is necessary to maintain the thermal balance of the whole system. This paper presents a graphical thermal model of proton exchange membrane fuel cell system based on energetic macroscopic representation and the thermal balance is analyzed using power chain. Then, the EMR-based control methodology is used to manage the operation temperature using inversion rules. Finally, the model is validated by MATLAB/Simulation.

**Keywords:** thermal model, proton exchange membrane fuel cell, energetic macroscopic representation, power chain, inversion rules

## 1. INTRODUCTION

Fuel cells play an important role in the power generation field due to their high energy conversion rate, diversified fuels, low environmental pollution, low noise, high reliability and good maintainability. The reaction process does not involve combustion, and the actual use efficiency is more than twice that of the ordinary internal combustion engine, and it has become the first choice for the green car. The proton exchange membrane fuel cell (PEMFC) is a power source that can potentially replace the internal combustion engine in vehicles of the future because of its suitable operating condition [1]. The energy efficiency of a PEMFC is about 50%, which indicates that about half of the chemical energy is converted to thermal energy in the electrochemical reaction. The internal heat source will

increase the operating temperature of the fuel cell. This will improve the output performance and catalyst activity, but the excessive temperature will cause the membrane dehydration and system attenuation. Therefore, the thermal management system is required to adjust the internal temperature of the fuel cell to maintain the heat balance of the stack.

Thermal model is essential for system thermal management, and numerous modeling methodologies are reviewed in [2], such as mechanistic models, empiric models, graphical models, and so on. A fuel cell system is complex and consists of many components, which is involving thermodynamics, hydrodynamics, electricity, electrochemistry and highly coupled with each other. The graphical approach is an effective means to handle the multi-physical, strong coupling and non-linear characteristics of fuel cell systems. The energetic macroscopic representation (EMR) is graphical method which can solve the above problems, and it uses arrows to establish the interactions between different parts [3]. The thermal model of fuel cell system can be easily organized by EMR elements defined in Appendix. In addition, the EMR model can be simply transformed to obtain the control structure though inversion rules [4].

The rest of this paper is organized as follows. Section 2 establishes the thermal model based on EMR, and the control structure is deduced in Section 3. Finally, the results analysis and conclusion are shown in Section 4 and 5, respectively.

## 2. THERMAL MODEL OF FUEL CELL SYSTEM

### 2.1 Structural description

Fuel cell systems are usually composed of fuel cell stack and balance-of-plant (BOP). The stack mainly consists of membrane electrodes assembly and bipolar

plates, which provides a site for electrochemical reactions. The BOP mainly provides good external working conditions for fuel cell, and it includes hydrogen supply subsystem, air supply subsystem, water and thermal subsystems. These subsystems play an important role in ensuring highly efficient and safe operations by providing proper working conditions.

As shown in Fig.1, a simplified fuel cell system structure is described with emphasis on the thermal subsystem or cooling circuit. The cooling components consist of a coolant pump, a reservoir, a heat exchanger and bypass valve, etc. The circuit provides two paths for coolant flow which is introduced an additional freedom by bypass valve compared with traditional cooling structure. The bypass valve allows coolant to flow from the stack outlet to the reservoir via bypass, or directly to flow into the heat exchanger for heat dissipation. Therefore, power consumption of the coolant circuit can be optimally controlled for a given heat rejection rate, which increases the overall system efficiency [5].

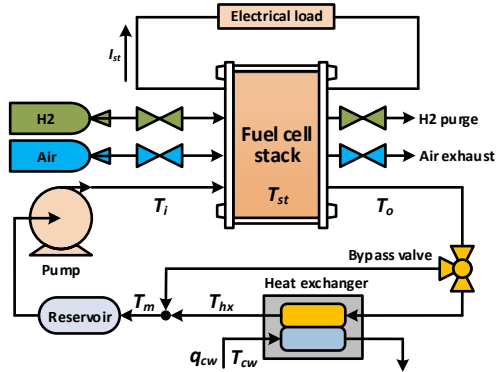


Fig 1 Simplified description of the fuel cell system

## 2.2 EMR-based modeling of thermal subsystem

Before modeling, several assumptions have been made on the thermal model as follows.

- The lumped modeling approach is employed without considering physical distribution effects.
- Ignore the enthalpy brought by the input and output gas and thermal radiation.
- Ignore the heat loss of the pump and pipes.

Based on the above assumptions, the thermal subsystem contains three parts: the thermogenic part, passive-cooling (P-cooling) part and active-cooling (A-cooling) part.

1) Thermogenic part: the fuel cell stack can be considered as a heat source for continuous heat production, which must be maintained at a suitable temperature though heat dissipation. Based on the definition of entropy resulting from the second law of thermodynamics, the rate of thermal change  $\dot{Q}$  is the

product of the rate of entropy change  $\dot{S}$  and its temperature  $T$  [6]:

$$\dot{Q} = \dot{S}T. \quad (1)$$

Therefore, the fuel cell stack considered as an entropy flow generator or source and the heat generated power is  $\dot{S}_{gen}T_{st}$ , which is represented by an oval pictogram in EMR with light green background and dark green contour as shown in Fig.2.

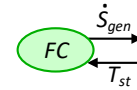


Fig 2 EMR of the fuel cell stack

2) P-cooling part: the definition is cooling via natural convection between the external surface area of the stack and the ambient. The rate of heat loss at the stack surface is related to the temperature difference and the heat transfer coefficient  $U_{st}$  and area  $A_{st}$ .

$$\dot{Q}_{amb} = \dot{S}_{amb}T_{amb} = (T_{amb} - T_{st})/R_{st} \quad (2)$$

where  $\dot{Q}_{amb}$  is the heat dissipated by ambient,  $\dot{S}_{amb}$  is the entropy flow into the ambient,  $T_{amb}$  and  $T_{st}$  are the ambient and stack temperature,  $R_{st}$  is the stack thermal resistance which is equal to  $1/U_{st}A_{st}$ . The EMR model is shown in Fig.3.

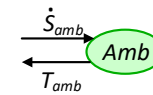


Fig 3 EMR of the ambient

3) A-cooling part: the definition is cooling via the addition external cooling stream to achieve heat dissipation through forced convection between stack and coolant. The heat consumption of A-cooling is implemented by a cooling circuit as shown in Fig.1, and only heat exchanger and reservoir are considered for heat absorbing. The pump and bypass are used to control the cooling process efficiently, and ignoring their heat loss.

The heat consumption power of the whole cooling circuit  $\dot{Q}_{cool}$  consists of the thermal power removed by heat exchanger  $\dot{Q}_{hx}$  and reservoir  $\dot{Q}_{rv}$

$$\dot{Q}_{cool} = \dot{S}_{cool}T_{st} = \dot{Q}_{hx} + \dot{Q}_{rv} \quad (3)$$

where  $\dot{S}_{cool}$  is the entropy flow into the cooling circuit.

The liquid-liquid type heat exchanger is employed to remove the heat from the hot coolant to chill water. It is assumed that the thermal inertia of the chill water is infinite, thus the chill water input temperature  $T_{cw}$

remains constant. The effectiveness-number of heat transfer units ( $\varepsilon$ - $NTU$ ) method is used to model the counter-flow type heat exchanger to obtain the outlet temperature of heat exchanger  $T_{hx}$ , which is deduced by formulas (4)-(6).

$$\varepsilon = \begin{cases} \frac{1 - e^{-NTU(1-C_R)}}{1 - C_R e^{-NTU(1-C_R)}} & C_R < 1 \\ \frac{NTU}{1 + NTU} & C_R = 1 \end{cases} \quad (4)$$

$$C_R = \frac{C_{\min}}{C_{\max}} = \frac{\min(q_{hx}c_{p,cl}, q_{cw}c_{p,cw})}{\max(q_{hx}c_{p,cl}, q_{cw}c_{p,cw})} \quad (5)$$

$$T_{hx} = T_o - \varepsilon(T_o - T_{cw}) \quad (6)$$

where  $T_o$  is the coolant inlet temperature,  $C_R$  is the capacity ratio,  $C_{\min}$ ,  $C_{\max}$  are the minimum and maximum specific heat flux respectively,  $q_{hx}$ ,  $q_{cw}$  are the coolant and chill water flux respectively,  $c_{p,cl}$ ,  $c_{p,cw}$  are the coolant and chill water specific heat capacity, respectively.

Therefore, the thermal power removed by heat exchanger is presented below:

$$\dot{Q}_{hx} = \dot{S}_{cw}T_{cw} - \dot{S}_{hxo}T_{hx} - \dot{S}_{hxi}T_o = q_{hx}c_{p,cl}(T_{hx} - T_o) \quad (7)$$

where,  $\dot{S}_{cw}$  is the entropy flow into the chill water,  $\dot{S}_{hxo}$  is the entropy flow out from the heat exchanger,  $\dot{S}_{hxi}$  is the entropy flow into the heat exchanger. The EMR of the model is shown in Fig.4.

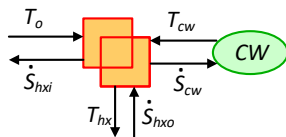


Fig 4 EMR of the heat exchanger

After the two coolants of different temperatures meet, the mixing temperature is determined by the two temperatures and the bypass valve opening width  $k$ . According to the specific heat capacity formula, the mixing temperature is calculated as follows:

$$T_m = kT_o + (1 - k)T_{hx} \quad (8)$$

The reservoir, as the site where the coolant is stored, has a large volume and a large heat capacity, so it has a large thermal inertia correspondingly, which can be expressed by the following formula

$$m_{rv}c_{p,rv} \frac{dT_i}{dt} = (\dot{S}_{rv} - \dot{S}_i)T_i + \dot{Q}_{rv} = q_{cl}c_{p,cl}(T_m - T_i) + \dot{Q}_{rv} \quad (9)$$

where  $m_{rv}$ ,  $c_{p,rv}$  are the mass and the specific heat capacity of the reservoir,  $\dot{S}_{rv}$ ,  $\dot{S}_i$  are the entropy flow into and out from the reservoir respectively,  $T_i$  is the coolant temperature at reservoir,  $q_{cl}$  is the total coolant flux.

Similar to P-cooling part, the thermal power removed by reservoir can be expressed as follows:

$$\dot{Q}_{rv} = \dot{S}_{rv2}T_{amb} = (T_{amb} - T_i) / R_{rv} \quad (10)$$

where  $\dot{S}_{rv2}$  is the entropy flow into the ambient from reservoir,  $R_{rv}$  is the reservoir thermal resistance. An accumulation block as shown in Fig.5 is employed to model the thermal inertia phenomenon of the reservoir.

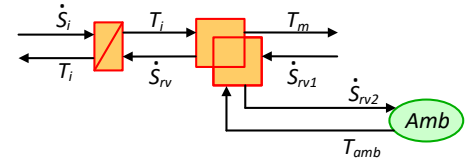


Fig 5 EMR of the reservoir

In conclusion, the stack temperature is determined by the above three parts, which is deduced by formula (11), and the complete EMR of the thermal subsystem is shown in Fig.6.

$$m_{st}c_{p,st} \frac{dT_{st}}{dt} = \dot{Q}_{gen} + \dot{Q}_{amb} + \dot{Q}_{cool} = (\dot{S}_{gen} + \dot{S}_{amb} + \dot{S}_{cool})T_{st} \quad (11)$$

where  $m_{st}$ ,  $c_{p,st}$  are the mass and the specific heat capacity of the fuel cell stack.

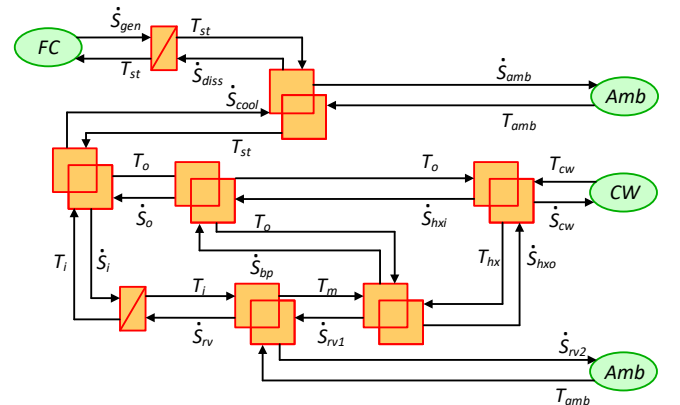


Fig 6 EMR model of the thermal subsystem

### 3. EMR-BASED CONTROL METHODOLOGY

The goal of the thermal subsystem is to maintain the stack temperature within an appropriate range and to ensure uniform temperature distribution. Therefore, it is necessary to control the stack outlet temperature and the temperature difference between the outlet and

the inlet. Specifically, the temperature difference is controlled by adjusting the flow rate of the pump, and the temperature of the stack inlet is controlled by adjusting the opening width of the bypass valve.

The control structure of the EMR can be easily obtained by inversion rules. The maximum control structure (MCS) of the thermal subsystem is shown in Fig.7.

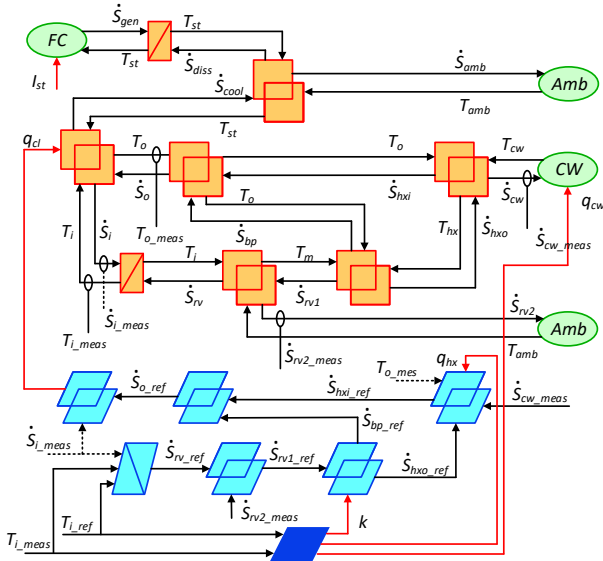


Fig 7 EMR and MCS of the thermal subsystem

The MCS is a step-by-step inversion of the EMR, but it some measurements are not physically possible and model limitations lead to modifications of the control [7]. Therefore, a practical control structure (PCS) naturally establishes by eliminating unrealistic problems, as shown in Fig.8.

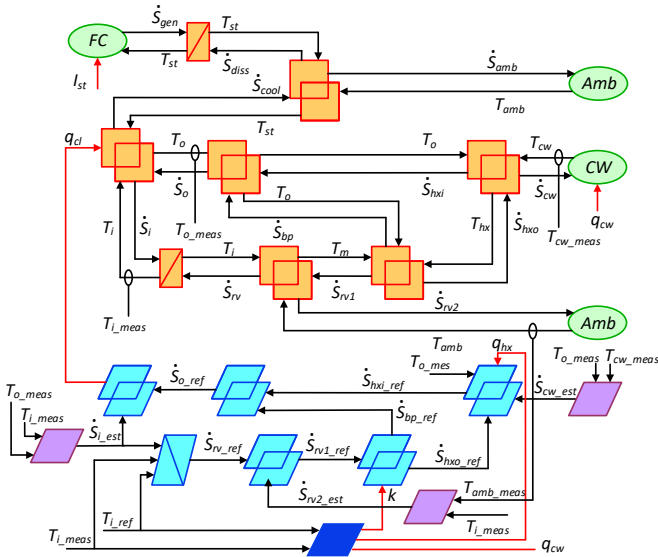


Fig 8 PCS of the thermal subsystem

#### 4. RESULTS AND DISCUSSION

The thermal subsystem modeling and temperature control are accomplished in MATLAB/Simulink software. The parameters used in this simulation are extracted from the literatures [8] and [9], which is not be repeated here. The stack and gas supply models are simplified in this paper, and heat production is determined by given current profile. The current profile and corresponding heating power are shown in Fig.9. Generally, the ideal operation temperature range of the stack is 333-353 K, taking the intermediate value, thus the reference temperature of the stack is set to 343 K. The outlet-inlet temperature difference is set to 7 K, which means the inlet objective temperature of stack is 336 K. Moreover, the ambient temperature is set to 298 K, and the inlet temperature and volume flows of the chill water are 298 K and 0.7 L/s, respectively.

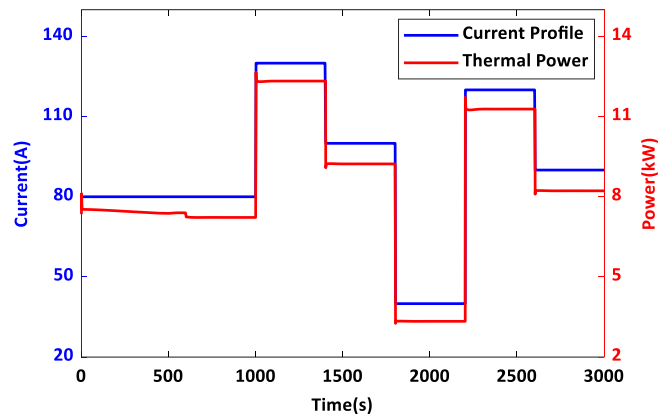


Fig 9 Current profile and thermal power of the stack

Fig.10 and 11 show the simulation results. In Fig.10, the total coolant flux and bypass valve opening width are plotted. Obviously, the fuel cell goes through two stages: start-up stage and normal operation stage. During the start-up stage, the coolant is circulated at a small flow rate, gradually increasing the temperature of the coolant. The bypass valve is fully opened and the coolant flows in a small circulation circuit to avoid the coolant passing through the heat exchanger which can reduces the heating time of the stack. In normal operation stage, the coolant flow rate changes with current and can be stabilized at a new operating point after a short period of time. The bypass valve will follow its change at the moment of current change, and then adjust itself stably. The overall opening width of the bypass valve is almost remained between 0.54-0.59. Fig.11 shows the temperature dynamic characteristics of the thermal subsystem. The four temperatures: stack temperature, stack inlet temperature, heat exchanger outlet temperature, and reservoir inlet temperature

have the same trend. When the current suddenly changes, the temperature will rise or fall accordingly, and then tend to stabilize. The above fours are stable at 343 K, 336 K, 331 K and 336.2 K, respectively.

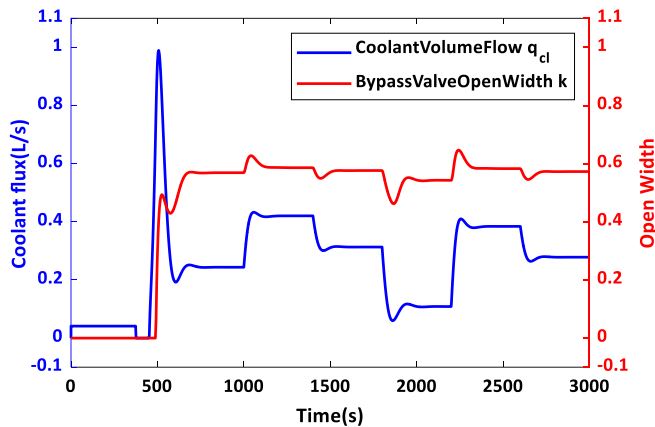


Fig 10 The coolant flux and bypass valve opening width

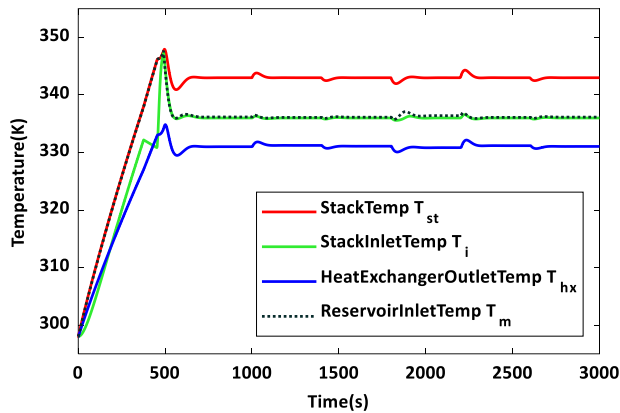


Fig 11 The dynamic temperature of the stack, the stack inlet, the heat exchanger outlet and the reservoir

Further, the direction of heat generated by the fuel cell will be analyzed. Already mentioned in the second section, the heat is consumed through three parts, namely heat exchange between the stack and environment (C1), heat dissipation by the heat exchanger (C2), and heat exchange between the reservoir and environment (C3).

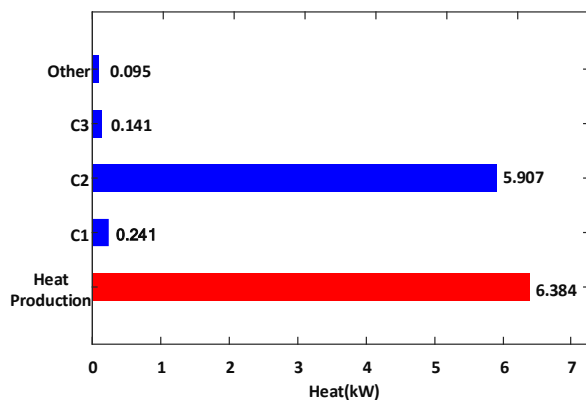


Fig 12 The heat production and consumption distribution

As shown in Fig.12, it exhibits the distribution of the heat production and consumption. The total heat produced by fuel cell is 6.384kW. The heat consumption by C1, C2, C3 are 0.241kW, 5.907kW, 0.141kW, respectively, and the percentage of each are 3.78%, 92.53%, 2.21%. It is not difficult to find that there is still residual heat, except for the above three heat dissipation. The residual heat is mainly used to raise the coolant temperature of reservoir and pipes in the initial stage.

## 5. CONCLUSION

The graphical modeling methodology is employed to establish the thermal subsystem of the fuel cell system based on EMR, which can clearly reflect the corresponding relationship between each component and EMR elements. According to the inversion rules, MCS is constructed step-by-step, and then obtained is obtained by eliminating unrealistic problems. The simulation is conducted with a 3000s current profile, and the results show that the temperature of stack has been controlled around 343 K with minor error which is not exceeding 2 K at operation stage. Through the analysis of heat production and heat dissipation, it is found that heat is mainly consumed by heat exchanger which is accounting for 92.53%, and heat dissipated by environment accounts for 5.99%.

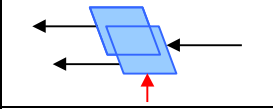
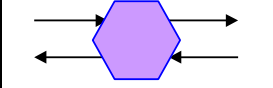
## ACKNOWLEDGEMENT

This work is supported by the National Natural Science Fund of China (Grant No. 61803359).

## APPENDIX

### EMR graphical representation

	Energy source (system terminals)
	Energy accumulation (energy storage)
	Mono-physical converter (energy conversion)
	Mono-physical coupling (energy distribution)
	indirect inversion (closed-loop control)
	direct inversion (open-loop control)

	Coupling inversion (distribution)
	Strategy (energy management)
	Model or estimator (any pictogram)

## REFERENCE

- [1] Zhao X, Li Y, Liu Z, Li Q, Chen W. Thermal management system modeling of a water-cooled proton exchange membrane fuel cell. *Int J Hydrogen Energy* 2015;40(7):3048-56.
- [2] Hissel D, Turpin C, Astier S, Boulon L, Bouscayrol A, Bultel Y, et al. A review on existing modeling methodologies for PEM fuel cell systems. *Fundamentals and developments of fuel cells conference*. 2008.
- [3] Bouscayrol A, Davat B, De Fornel B, François B, Hautier J, Meibody-Tabar F, et al. Multi-converter multi-machine systems: application for electromechanical drives. *Eur Phys J-Appl Phys*. 2000;10(2):131-47.
- [4] Barrre P, Bouscayrol A, Delarue P, Dumetz E, Giraud F, Hautier J-P, et al. Inversion-based control of electromechanical systems using causal graphical descriptions. *IECON 2006-32nd Annual Conference on IEEE Industrial Electronics: IEEE*; 2006. p. 5276-81.
- [5] Ahn J. Control and analysis of air, water, and thermal systems for a polymer electrolyte membrane fuel cell [dissertation]. Alabama: Auburn University; 2011.
- [6] Shoureshi R, McLaughlin K. Analytical and experimental investigation of flow-reversible heat exchangers using temperature-entropy bond graphs. *American Control Conference, 1983. Proceedings of the 1983. IEEE*; 1983. p. 1299-304.
- [7] Boulon L, Hissel D, Bouscayrol A, Pera MC. From Modeling to Control of a PEM Fuel Cell Using Energetic Macroscopic Representation. *Ind Electron, IEEE Trans* 2010;57(6):1882-91.
- [8] Hu P, Cao G, Zhu X, Hu M. Coolant circuit modeling and temperature fuzzy control of proton exchange membrane fuel cells. *Int J Hydrogen Energy* 2010; 35(17):9110-23.
- [9] Pukrushpan JT, Stefanopoulou AG, Peng H. Control of fuel cell power systems: principles, modeling, analysis and feedback design. London: Springer; 2004.